Version 1.3 as of July 18, 2006

Combined DØ and CDF Upper Limits on Standard Model Higgs Boson Production

The TEVNPH Working Group*

for the DØ and CDF Collaborations

We combine the results of the CDF and DØ searches for Standard Model Higgs boson production. The data are recorded in $p\bar{p}$ collisions produced at the Tevatron with $\sqrt{s} = 1.96$ TeV, with 260-950 pb^{-1} collected at DØ and 290-1000 pb^{-1} collected at CDF . The 95% CL upper limits are a factor of 14.5(3.9) higher than the Standard Model cross section at m_H =115(160) GeV/c^2. This result significantly extends the individual limits for each experiments.

I. INTRODUCTION

As the mechanism for electroweak-symmetry breaking in the Standard Model (SM) remains undiscovered, the search for a SM Higgs boson represents a significant portion of the Tevatron physics program. Both DØ and CDF have recently reported on a search for a SM Higgs boson combining searches in different final states and production modes[1, 2]. At this time, CDF and DØ have recorded sufficient integrated luminosity to motivate a combination of search results.

In this note, we present and combine results on direct searches for SM Higgs bosons in $p\bar{p}$ collisions at $\sqrt{s} = 1.96$ TeV at both the CDf and DØ experiments. These are searches for Higgs bosons produced in association with vector bosons ($p\bar{p} \rightarrow W/ZH \rightarrow \ell\nu b\bar{b}/\nu\nu b\bar{b}$ or $p\bar{p} \rightarrow WH \rightarrow WW^+W^-$) or produced via gluon-gluon fusion ($p\bar{p} \rightarrow H \rightarrow W^+W^-$). The searches were performed with data corresponding to integrated luminosities ranging from 289-1000 pb^{-1} at CDF and 261-950 pb^{-1} at DØ . The searches are separated into nine final states, referred to as analyses in the following. In order to ensure proper combination of signals, the analyses were designed to be mutually exclusive after analysis selections. The selection procedure for each analysis is detailed in each experiment's individual combination notes, and briefly described below.

II. ACCEPTANCE, BACKGROUNDS, AND LUMINOSITY

Selections are similar amongst corresponding CDF and DØ analyses. In the case of the $WH \rightarrow \ell\nu b\bar{b}$ analyses, an isolated lepton (electron or muon) and at least two jets are required, with one or more jets tagged as originating from b-quarks. These two tagged selections are separated into orthogonal groups and are referred to as exclusive single-tag (ST) and double-tag (DT) selections. Finally, events must display a significant imbalance of momentum in the plane transverse to the beam axis (referred to as missing energy or $\not\!\!E_T$). Events with additional isolated leptons are vetoed. For the $ZH \rightarrow \nu\nu b\bar{b}$ analyses, the selection is similar except all events with isolated leptons are vetoed and stronger multijet background suppression techniques are applied. For the CDF $ZH \rightarrow \nu\nu b\bar{b}$ analysis, the ST and DT samples are combined to form one single sample requiring at least one b-tagged jet. As there is a sizeable amount of $WH \rightarrow \ell\nu b\bar{b}$ signal that can mimic the $ZH \rightarrow \nu\nu b\bar{b}$ final state when the lepton is undetected, the DØ analyses include this as a separate search, referred to as $WH \rightarrow \not\ell\nu b\bar{b}$. In the $WH \rightarrow \ell\nu b\bar{b}$ and $ZH \rightarrow \nu\nu b\bar{b}$ analyses, the final variable used for limit setting is the invariant dijet mass. For the $H \rightarrow W^+W^-$ analyses, a large $\not\!\!E_T$and two opposite-signed isolated leptons (electrons or muons) are selected, defining three final states (e^+e^-, $e^\pm\mu^\mp$, and $\mu^+\mu^-$). Due to the neutrinos in the final state, the Higgs mass cannot be directly reconstructed and the final variable used is the difference in φ between the two final state leptons. The DØ experiment also contributes three $WH \rightarrow WW^+W^-$ analyses, where the associated W boson and the same-charged W boson from the Higgs decay are required to decay semi-leptonically, thus defining six final states where all decays of the third W boson are included. In this case of this analysis, the final variable is a likelihood discriminant formed from several topological variables.

All Higgs signals are simulated using PYTHIA v6.202[3] using CETQ5L[4] leading order parton distribution functions. The signal cross sections are normalized to next-to-next-to-leading order calculations[5, 6] and branching ratios are calculated using HDECAY[7]. For both CDF and DØ , events from multijet backgrounds (QCD production)

* The Tevatron New-Phenomena and Higgs working group can be contacted at TEVNPHWG@fnal.gov. The members of the TEVNPH working group and the physicists who performed this combination are: .

TABLE I: The luminosity, expected signal, expected background, and observed data for the CDF analyses. Also included is the Higgs mass for which each set of numbers are derived. The numbers of expected events are determined for $0 \leq m_{jj} \leq 200$ GeV/c^2 for $H \to b\bar{b}$ analyses, and $0 \leq \Delta\varphi(\ell_1, \ell_2) \leq \pi$ Rad for $H \to W^+W^-$ analyses.

	$WH \to \ell\nu b\bar{b}$ DT(ST)	$ZH \to \nu\nu b\bar{b}$	$H \to W^+W^- \to \ell^\pm\nu\ell^\mp\nu$
Luminosity (pb^{-1})	1000	289	360
Expected Signal (evts)	0.50 (1.47)	0.23	0.84
Expected Background (evts)	40.2 (366.3)	19.6	13.8
Data (evts)	36 (390)	19	18
m_H (GeV/c^2)	115	110	160
Reference	[12]	[13]	[14]

TABLE II: The luminosity, expected signal, expected background, and observed data for the DØ $H \to b\bar{b}$ analyses. The number of expected signal, background, and data are determined for $0 \leq m_{jj} \leq 200$ GeV/c^2.

	$WH \to e\nu b\bar{b}$ DT(ST)	$WH \to \mu\nu b\bar{b}$ DT(ST)	$WH \to \not\ell\nu b\bar{b}$ DT(ST)	$ZH \to \nu\nu b\bar{b}$ DT(ST)
Luminosity (pb^{-1})	371	385	261	261
Expected Signal (evt)	0.19 (0.22)	0.11 (0.12)	0.18 (0.20)	0.24 (0.26)
Expected Background (evts)	14.6 (58.3)	10.2 (46.8)	25.2 (87.3)	25.2 (87.3)
Data (evts)	14 (57)	8 (48)	23 (98)	23 (98)
m_H (GeV/c^2)	115	115	115	115
Reference	[15]	[15]	[16]	[16]

are measured in data, but with different methods. For the CDF analyses, backgrounds were generated by PYTHIA, ALPGEN[8], and HERWIG[9]. For the DØ analyses, backgrounds were generated by PYTHIA, ALPGEN, and COMPHEP[10], with PYTHIA providing parton-showering and hadronization for all. Background processes were either normalised using experimental data or using the next-to-leading order calculations from MCFM[11] in all possible cases.

The values of the integrated luminosity, expected signal, expected background, and observed data are given in Table I for CDF analyses and Tables II-IV for DØ analyses. The expected numbers of events are integrated in the range $0 \leq m_{jj} \leq 200$ GeV/c^2 for $H \to b\bar{b}$ analyses, $0 \leq \Delta\varphi(\ell_1, \ell_2) \leq \pi$ Rad for $H \to W^+W^-$ analyses, and $0 \leq Discrim \leq 1$ for the $WH \to WW^+W^-$ analyses. The table also includes the value of the Higgs mass for which each set of numbers is derived.

III. COMBINATION PROCEDURES

We combine results using two different methods, to gain confidence that the result does not depend on the details of the statistical method used. In both methods, the final variables are treated as histograms binned according to the experimental resolution of the variable, rather than a single, fully-integrated value. Systematic uncertainties are treated as uncertainties on the expected numbers of signal and background events for each analysis, not the outcomes of the limit calculations. Both methods use likelihood calculations based upon Poisson probabilities.

TABLE III: The luminosity, expected signal, expected background, and observed data for the DØ $H \to W^+W^-$ analyses. The number of expected signal, background, and data are determined for $0 \leq \Delta\varphi(\ell_1, \ell_2) \leq \pi$ Rad

	$H \to W^+W^- \to e^+\nu e^-\nu$	$H \to W^+W^- \to e^\pm\nu\mu^\mp\nu$	$H \to W^+W^- \to \mu^+\nu\mu^-\nu$
Luminosity (pb^{-1})	950	950	950
Expected Signal (evts)	0.64	1.50	0.54
Expected Background (evts)	11.4	28.1	10.5
Data (evts)	11	18	10
m_H (GeV/c^2)	160	160	160
Reference	[17]	[17]	[18]

TABLE IV: The luminosity, expected signal, expected background, and observed data for the DØ $WH \to WW^+W^-$ analyses. The number of expected signal, background, and data are determined for $0 \leq \Delta\varphi(\ell_1, \ell_2) \leq \pi$ Rad

	$WW^+W^- \to e^\pm\nu e^\pm\nu$	$WW^+W^- \to e^\pm\nu\mu^\pm\nu$	$WW^+W^- \to \mu^\pm\nu\mu^\pm\nu$
Luminosity (pb^{-1})	384	368	363
Expected Signal (evts)	0.043	0.101	0.066
Expected Background (evts)	15.4	7.0	12.5
Data (evts)	15	7	12
m_H (GeV/c^2)	155	155	155
Reference	[19]	[19]	[19]

A. Frequentist Method

The first technique uses the CL_s method with a log-likelihood ratio (LLR) test statistic[1], as given by:

$$\chi_n = 2\sum_{i=1}^{N_C}\sum_{j=1}^{Nbins}(s_{ij} - n_{ij}\mathrm{Log}(1 + \mathrm{s_{ij}/b_{ij}})) \tag{1}$$

where the first sum is over the number of channels (N_C), the second sum is over histogram bins and the value n is given by the hypothesis being probed. The value of CL_s is then defined as the normalization of the signal+background hypothesis (CL_{s+b}) by the background-only hypothesis (CL_b). This construction reduces the ambiguity of "unphysical" results ($e.g.$, negative cross section limits) and distinctly separates the estimator from the quantity being probed.

B. Bayesian Method

The second method is a Bayesian technique[2]. Because there is nothing known about the Higgs production cross section, this method assigns a flat prior to the total number of Higgs events $R \times s_{tot}$, instead of the cross section. For a given Higgs mass hypothesis, the combined likelihood is a product of the likelihoods in the individual channels, each of which is a product over histogram bins:

$$\mathcal{L}(R, \vec{s}, \vec{b}|\vec{n}) = \prod_{i=1}^{N_C}\prod_{j=1}^{Nbins}\mu_{ij}^{n_{ij}}e^{-\mu_{ij}}/n_{ij}! \tag{2}$$

where the first product is over the number of channels (N_C), and the second product is over histogram bins with observed data events (n_{ij}) in either dijet mass for WH and ZH, $\Delta\varphi$ of two leptons in $H \to W^+W^-$, or the likelihood discriminant in $WH \to WW^+W^-$. The parameters that contribute to the expected bin contents are $\mu_{ij} = R\times s_{ij}+b_{ij}$ for the channel i and the histogram bin j. The posterior density function is then integrated over all parameters with correlations except R, and a 95% credibility level upper limit on R is obtained by calculating the 95^{th} percentile of the resulting distribution.

C. Systematic Uncertainties

The systematic uncertainties for the background rates are generally several times larger than the signal expectation and are thus an important factor in the calculation of limits. As such, each systematic uncertainty is folded into the signal and background expectations via Gaussian distribution according to its size. The Gaussian values are sampled once for each Poisson MC trial (pseudo-experiment). Correlations between systematic sources are carried through in the calculation. The systematic uncertainties differ between experiments and analyses for both the signals and backgrounds. Detailed discussions of these considerations are included in the individual analysis notes. Here we will consider only the largest contributions and the correlations amongst and within the two experiments.

TABLE V: The breakdown of systematic uncertainties for each individual CDF analysis. All positive-signed uncertainties within a group are considered 100% correlated across channels. Values with negative signs are considered uncorrelated.

Source	$WH \to \ell\nu b\bar{b}$ ST	$WH \to \ell\nu b\bar{b}$ DT	$ZH \to \nu\nu b\bar{b}$	$H \to W^+W^-$
Luminosity (%)	6.0	6.0	6.0	6.0
b-Tag Scale Factor (%)	5.3	16.0	6.3	0
Lepton Identification (%)	2.0	2.0	2.0	3.0
Jet Energy Scale (%)	3.0	3.0	8.0	1.0
I(S)R+PDF (%)	4.0	10.0	2.0	5.0
Trigger (%)	0	0	0.02	0
Backgrounds				
Heavy Flavor (%)	33.0	34.0	0	0
Mistag (%)	22.0	15.0	16.0	0
Top (%)	13.5	20.0	18.0	0
QCD (%)	17.0	20.0	-34.0	0
Diboson (%)	16.0	25.0	18.0	11.0
Others (%)	0	0	0	-(12-18)

1. *Correlated Systematics*

The uncertainty on the measurement of the integrated luminosity is 6% (CDF) and 6.5% (DØ). Of this value, 4% arises from the uncertainty on the inelastic $p\bar{p}$ scattering cross section, which is correlated between CDF and DØ . The uncertainty on the production rates for top-quark processes ($t\bar{t}$ and single-top) and electroweak processes (WW, WZ, and ZZ) are also taken as correlated between the two experiments. As the methods of measuring the multijet (qcd) backgrounds differ between CDF and DØ , there is no correlation assumed for this uncertainty.

2. *CDF Systematics*

The dominant systematic uncertainties for the CDF analyses are shown in Table V. For the CDF $H \to b\bar{b}$ analyses, the largest signal rate uncertainties arise from the b-tagging scale factor (5.3-16%), jet energy scale (3-8%), and Monte Carlo (MC) modeling (2-10%). For the CDF $H \to W^+W^-$ analyses, the largest contributing uncertainty comes from MC modeling (5%). For the backgrounds, the uncertainties on the expected rate range from 11-34% (varying by background type). Because the largest background contributions are measured using data, the uncertainties are treated as uncorrelated for the $H \to b\bar{b}$ channels. For the $H \to W^+W^-$ channel the luminosity uncertainty is taken to be correlated between signal and background. The differences between treating the remaining uncertainties to be correlated or uncorrelated is less than 5%.

3. *DØ Systematics*

The dominant systematic uncertainties for the DØ analyses are shown in Table VI. The DØ $H \to b\bar{b}$ analyses have an uncertainty on the b-tagging rate of 5-7% per tagged jet. These analyses also have an uncertainty on the jet measurement and acceptances of 6-9% (jet identification (jet ID), energy scale, and jet smearing). For the DØ $H \to W^+W^-$ and $WH \to WW^+W^-$ analyses, the largest uncertainties are associated with lepton measurement and acceptances. These values range from 3-6% depending on the final state. The largest contributing factor for all analyses is the uncertainty on the background cross sections at 6-15%. These systematics are assumed to apply to both signal and background. All systematic uncertainties arising from the same source are taken to be correlated between signals and backgrounds, as detailed in Table VI.

IV. COMBINED RESULTS

Using the combination procedures outlined above, we are able to derive combined limits on SM Higgs boson production $\sigma \times BR * (H \to X)$ in $p\bar{p}$ collisions at $\sqrt{s} = 1.96$ TeV. Figure 1 gives the log-likelihood ratio (LLR)

TABLE VI: List of leading correlated systematic uncertainties for the DØ analyses. The values for the systematic uncertainties are the same for the $ZH \rightarrow \nu\nu b\bar{b}$ and $WH \rightarrow \not\ell\nu b\bar{b}$ channels. All uncertainties within a group are considered 100% correlated across channels. The correlated systematic uncertainty on the background cross section (σ) is itself subdivided according to the different background processes in each analysis.

Source	$WH \rightarrow e\nu b\bar{b}$ DT(ST)	$WH \rightarrow \mu\nu b\bar{b}$ DT(ST)	$ZH \rightarrow \nu\nu b\bar{b}$ DT(ST)	$H \rightarrow W^+W^-$, $WH \rightarrow WW^+W^-$
Luminosity (%)	6.5	6.5	6.5	6.5
Jet Energy Scale (%)	4	5	6	3
Jet ID (%)	6.8	6.8	7.1	0
Electron ID (%)	6.6	0	0	2.3
Muon ID (%)	0	4.9	0	7.7
b-Jet Tagging (%)	8.5(5)	8.5(5)	9.6(6.7)	0
Background σ (%)	6-33	6-25	6-33	6-33

distributions for the combined analyses. Included in this figure are the LLR values for the background-only hypothesis (LLR$_b$), the signal+background hypothesis (LLR$_{s+b}$), and the observed data (LLR$_{obs}$). The shaded bands represent the 1-σ and 2-σ regions for LLR$_b$. The LLR value is a joint test statistic given by

$$LLR_n = \Sigma_i n_i \mathrm{Log}(1 + s_i/b_i) \tag{3}$$

where n_i denotes the hypothesis being tested (*e.g.*, background-only or observed data) and the sum runs over the number of bins (or analyses) being combined. This value can be interpreted as follows:

- The separation between LLR$_b$ and LLR$_{s+b}$ provides a measure of the overall search power of the analysis. This is the ability of the analysis to separate the $s + b$ and $b-$only hypotheses.
- The width of the LLR$_b$ distribution (shown here as 1-σ and 2-σ bands) gives an estimate of how sensitive the analysis is to a signal-like fluctuation in data in the presence of systematic uncertainties. For example, when a 1-σ background fluctuation is large compared to the signal expectation, the analysis sensitivity is limited.
- The value of LLR$_{obs}$ indicates whether the data distribution appears to be more signal-like or background-like, depending on its position with respect to the LLR$_{s+b}$ and LLR$_b$ values. Furthermore, the significance of any departures of LLR$_{obs}$ from LLR$_b$ can be evaluated by the width of the LLR$_b$ distribution.

To facilitate model transparency and to accommodate analyses with different degrees of sensitivity, we present our results in terms of the ratio of limits set to the SM cross sections as a function of Higgs mass. A ratio value of unity or less would indicate a Higgs mass excluded at 95% CL. The expected (median) and observed 95% cross section upper limits for the combined CDF and DØ analyses are shown in Figure 2. The observed and expected limit ratios are listed for select Higgs masses in Table VII, with observed(expected) values of 14.5(11.3) at $m_H = 115$ GeV/c^2 and 3.9(5.0) at $m_H = 160$ GeV/c^2.

These results represent an improvement in search sensitivity over each individual experiment, which set find observed(expected) limit ratios of 16.3(17.7) for DØ and 23.1(15.4) for CDF at $m_H = 115$ GeV/c^2 and of 4.3(6.0) for DØ and 11.5(10.3) for CDF at $m_H = 160$ GeV/c^2.

APPENDIX A: FOR CDF AND DØ INTERNAL REVIEW

Figure 3 shows the comparison of the limits derived using the CL_s method and the Bayesian technique to derive the combined Tevatron Higgs cross section limit. The two methods agree within 10%. At low mass the Bayesian procedure gives better limits while at high masses the CL_s method yields a better limit.

[1] DØ Collaboration, Conference Note 5056, "Limits on Standard Model Higgs Boson Production"
[2] CDF Collaboration, "Combined Upper Limit on Standard Model higgs Boson Production at CDF", CDF/ANAL/EXOTIC/PUBLIC/8326
[3] T. Sjostrand, L. Lonnblad and S. Mrenna, "PYTHIA 6.2: Physics and manual," [arXiv:hep-ph/0108264]

[4] H. L. Lai *et al.*, *Improved Parton Distributions from Global Analysis of Recent Deep Inelastic Scattering and Inclusive Jet Data*, Phys. Rev D **55** (1997) 1280

[5] S. Catani, D. de Florian, M. Grazzini and P. Nason, "Soft-gluon resummation for Higgs boson production at hadron colliders," JHEP **0307**, 028 (2003), [arXiv:hep-ph/0306211]

[6] K. A. Assamagan *et al.* [Higgs Working Group Collaboration], "The Higgs working group: Summary report 2003," [arXiv:hep-ph/0406152]

[7] A. Djouadi, J. Kalinowski and M. Spira, "HDECAY: A program for Higgs boson decays in the standard model and its supersymmetric extension," Comput. Phys. Commun. **108**, 56 (1998) [arXiv:hep-ph/9704448]

[8] M. L. Mangano, M. Moretti, F. Piccinini, R. Pittau and A. D. Polosa, "ALPGEN, a generator for hard multiparton processes in hadronic collisions," JHEP **0307**, 001 (2003) [arXiv:hep-ph/0206293]

[9] G. Corcella *et al.*, "HERWIG 6: An event generator for hadron emission reactions with interfering gluons (including supersymmetric processes)," JHEP **0101**, 010 (2001) [arXiv:hep-ph/0011363]

[10] A. Pukhov *et al.*, "CompHEP: A package for evaluation of Feynman diagrams and integration over multi-particle phase space. User's manual for version 33," [arXiv:hep-ph/9908288]

[11] J. Campbell and R. K. Ellis, "Next-to-leading order corrections to W + 2jet and Z + 2jet production at hadron colliders," Phys. Rev. D **65**, 113007 (2002), [arXiv:hep-ph/0202176]

[12] CDF 1 fb^{-1} WH result.

[13] CDF Collaboration, "Search for the Standard Model Higgs Boson in the $ZH \rightarrow \nu\nu b\bar{b}$ channel," CDF/ANAL/EXOTIC/PUBLIC/7983

[14] CDF Collaboration, "Search for the Standard Model Higgs Boson in the $gg \rightarrow H \rightarrow WW^*$ Dilepton Channel with 360 pb^{-1} ," CDF/ANAL/EXOTIC/PUBLIC/7893

[15] DØ Collaboration, "Search for WH Production at $\sqrt{s} = 1.96$ TeV," DØ Conference Note 5054

[16] DØ Collaboration, "A Search for the Standard Mondel Higgs boson using the $ZH \rightarrow \nu\nu b\bar{b}$ channel in $p\bar{p}$ Collisions at $\sqrt{s} = 1.96$ TeV," DØ Conference Note 5060

[17] DØ Collaboration, "Search for the Higgs boson in $H \rightarrow WW^* \rightarrow l^+l^-(ee, e\mu)$ decays with 950 pb^{-1} at DØ in Run II," DØ Conference Note 5063

[18] DØ HWW mumu result. Conference Note XXXX

[19] DØ Collaboration, "A Search for Associated Higgs Boson Production WH -¿ WWW* -¿ l+-nu l'+-nu' + X in ppbar collisions at $\sqrt{s} = 1.96$ TeV," DØ Conference Note 5021

TABLE VII: Expected (median) and observed 95% CL cross section ratios for the combined CDF and DØ analyses.

	100 GeV/c^2	115 GeV/c^2	120 GeV/c^2	140 GeV/c^2	160 GeV/c^2	180 GeV/c^2	200 GeV/c^2
Expected	7.8	11.4	12.5	9.4	5.0	7.6	15.7
Observed	9.1	15.0	14.9	8.9	3.9	6.1	12.4

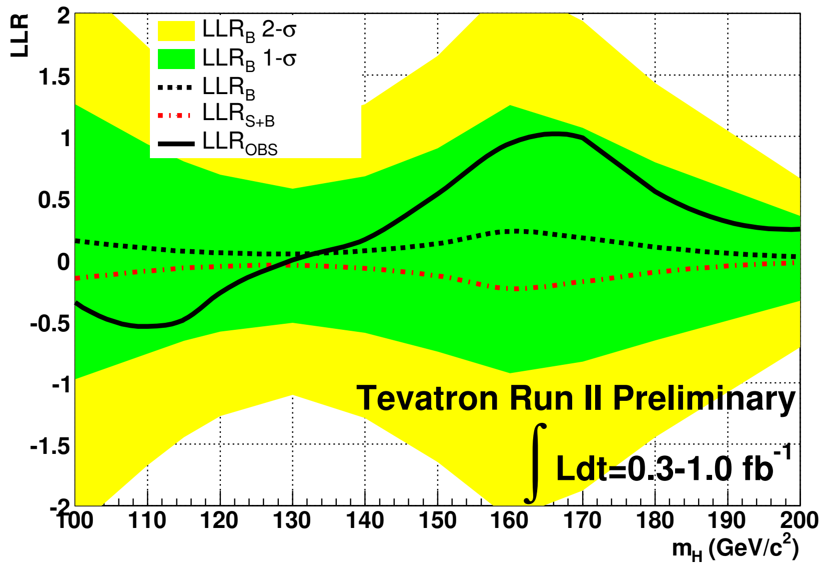

FIG. 1: Log-likelihood ratio distribution for the combined CDF and DØ analyses. Shown in the plot are the LLR$_b$ (background-only hypothesis), LLR$_{s+b}$ (signal+background hypothesis), LLR$_{obs}$ (observed LLR value), and the 1-σ and 2-σ bands for the LLR$_b$ distribution.

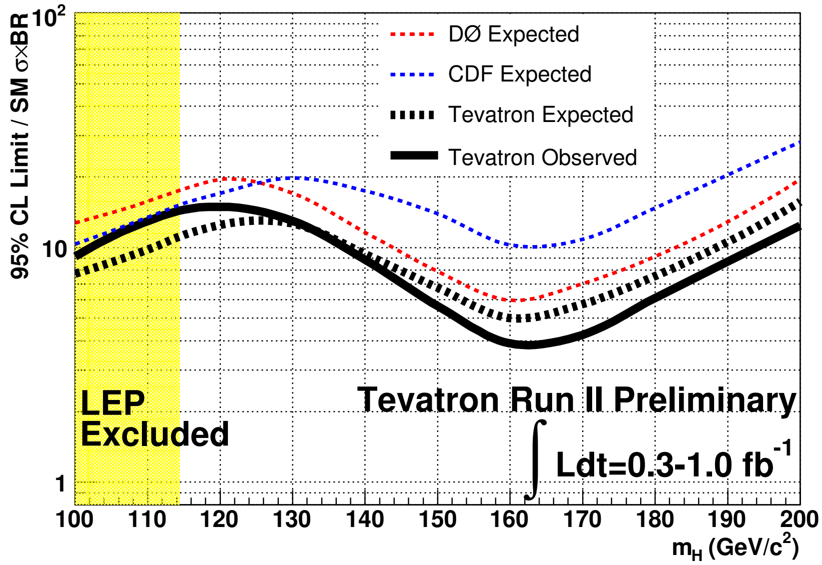

FIG. 2: Expected (median) and observed 95% CL cross section ratios for the combined CDF and DØ analyses. Also shown are the expected 95% CL ratios for the CDF and DØ experiments alone.

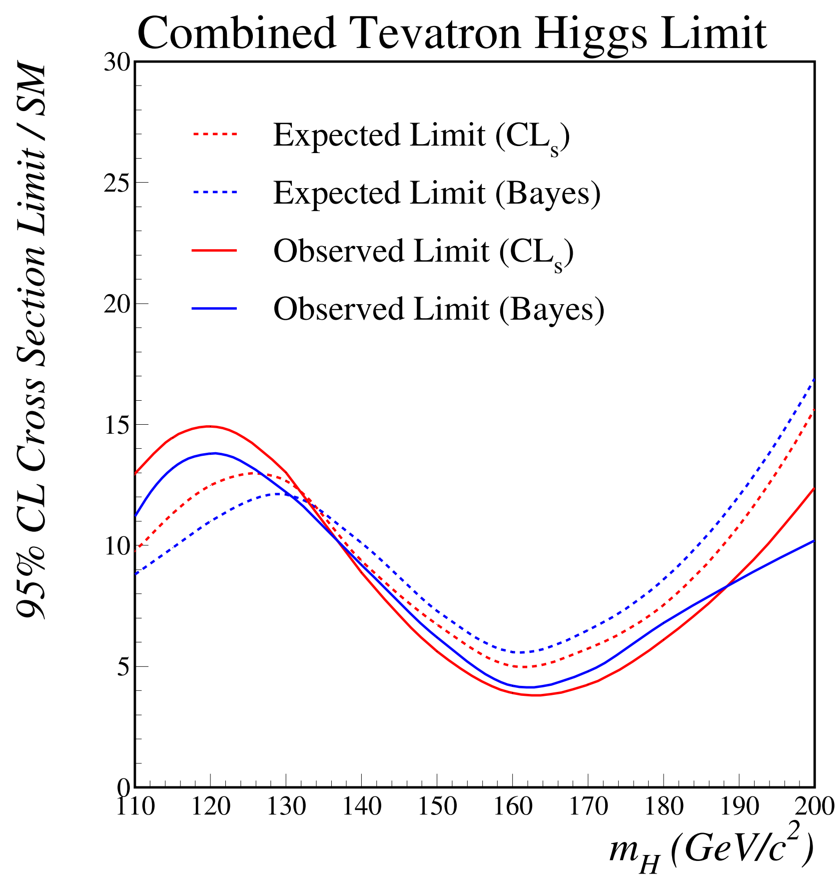

FIG. 3: Shown are the observed and expected limit on the ratio of the Higgs production cross section divided by the Standard Model using two different statistical treatments. The red lines show the limits derived using the CLs method and the blue show those derived using the Bayesian technique. The dashed lines show the expected and the solid lines the observed limits.